

Statistical properties of the s-process nucleus ^{87}Kr from inverse kinematic reactions

V. W. Ingeberg,^{1,*} S. Siem,^{1,†} M. Wiedeking,^{2,‡} K. Sieja,^{3,4} F. Zeiser,¹ D. L. Bleuel,⁵ C. P. Brits,^{2,6} T. D. Bucher,² T. S. Dinoko,² J. L. Easton,^{2,7} A. Görzen,¹ M. Guttormsen,¹ P. Jones,² B. V. Kheswa,⁸ N. A. Khumalo,² A. C. Larsen,¹ E. A. Lawrie,² J. J. Lawrie,² S. N. T. Majola,^{2,9} K. L. Malatji,^{2,6} L. Makhathini,^{2,6} B. Maqabuka,^{2,7} D. Negi,² S. P. Noncolela,^{2,7} P. Papka,^{2,6} E. Sahin,¹ R. Schwengner,¹⁰ G. M. Tveten,¹ and B. R. Zikhali^{2,9}

¹Department of Physics, University of Oslo, N-0316 Oslo, Norway

²iThemba LABS, P.O. Box 722, 7129 Somerset West, South Africa

³Université de Strasbourg, IPHC, 23 rue du Loess 67037 Strasbourg, France

⁴CNRS, UMR7178, 67037 Strasbourg, France

⁵Lawrence Livermore National Laboratory, 7000 East Avenue, Livermore, California 94550-9234, USA

⁶Department of Physics, Stellenbosch University, Private Bag X1, Matieland, 7602, South Africa

⁷Department of Physics, University of the Western Cape, P/B X17 Bellville 7535, South Africa

⁸Department of Physics, University of Johannesburg,
P.O. Box 524, Auckland Park 2006, South Africa

⁹Department of Physics, University of Zululand, Private Bag X1001, KwaDlangezwa 3886, South Africa

¹⁰Institut für Strahlenphysik, Helmholtz-Zentrum Dresden-Rossendorf, 01314 Dresden, Germany

A novel technique for extracting the γ -ray strength function (γ SF) and nuclear level density (NLD) from inverse kinematics experiments is presented, which allows for measurements of these properties, across a vast range of previously inaccessible nuclei. Proton- γ coincidence events from the $d(^{86}\text{Kr}, p\gamma)^{87}\text{Kr}$ reaction were measured at iThemba LABS, and the γ SF and NLD in ^{87}Kr obtained with the Oslo Method. The γ SF and NLD are important input parameters to Hauser-Feshbach calculations to constrain (n, γ) cross sections of nuclei for which these cannot be measured directly. The extracted γ SF and NLD are used to constrain the $^{86}\text{Kr}(n, \gamma)^{87}\text{Kr}$ cross section which is an important reaction for the ^{87}Rb production in the *s*-process. The nature of the low-energy region of the γ SF is explored through comparison to shell model calculations.

One of the major mechanisms to explain the production of nearly half of the nuclei heavier than iron is the slow neutron-capture process (*s*-process) which is subdivided into the main and weak *s*-processes [1]. The former occurs during the hydrostatic stellar burning phases of low-mass stars in their asymptotic giant branch phase [2] and mainly produces $90 < A < 210$ nuclei. The weak *s*-process takes place in massive stars during core He- or shell C-burning and primarily produces $A < 90$ nuclei [3]. In massive stars neutrons are produced through the $^{22}\text{Ne}(\alpha, n)$ reaction, with neutron densities of $10^{11} - 10^{12}$ cm $^{-3}$ for shell C-burning and 10^6 cm $^{-3}$ for core He-burning [4, 5].

Branching nuclei are very sensitive to the neutron density and temperature environments and hence provide detailed insight into *s*-process nucleosynthesis. ^{85}Kr is such a branching nucleus with a ground state half life of 10.74h and, depending on the neutron density, can either produce ^{85}Rb via β^- decay or ^{86}Kr through the (n, γ) reaction [6]. The situation is further complicated by a 4.48h isomer in ^{85}Kr which primarily β^- decays to ^{85}Rb [7]. In low-neutron density environments the $^{85}\text{Kr}(n, \gamma)$ reaction cannot effectively compete with the β^- decay of ^{85}Kr [4]. In comparison, high-neutron densities strongly favor the production of ^{87}Rb via the *s*-process reactions $^{85}\text{Kr}(n, \gamma)^{86}\text{Kr}(n, \gamma)^{87}\text{Kr}$ and modify the isotopic composition between ^{85}Rb and ^{87}Rb . The Rb isotopic mix and total abundance is extremely sensitive to the neutron density and has been shown to differ by an order of magnitude depending on whether a low-neutron or high-

neutron density is present. The implications are significant since the relative abundance of Rb to other elements such as Sr, Y, or Zr can be used to estimate the average neutron sensitivity of the *s*-process and from this conclusions can be drawn on the mass of the star [4, 8].

Kr isotopes are particularly interesting because they are found in pre-solar grains [9, 10], which originated prior to the formation of the solar system, and their isotopic abundances can be measured with high accuracy. From these carbonaceous grains it is apparent that the calculated ^{86}Kr abundance suffers from large uncertainties, strongly affected by the ^{85}Kr branching nucleus [11]. During the weak *s*-process $^{85}\text{Kr}(n, \gamma)$ and $^{86}\text{Kr}(n, \gamma)$ are key reactions in the production and destruction of ^{86}Kr [12]. The global and local impact of the $^{86}\text{Kr}(n, \gamma)$ reaction on the final abundance uncertainties has been identified as one of the key reactions for the ^{86}Kr production in the ^{13}C pocket and to produce ^{87}Rb in the thermal pulse [13]. In a rotating stellar environment the weak *s*-process is enhanced [14] and the $^{86}\text{Kr}(n, \gamma)$ reaction is also found to be a key reaction to understand the production mechanism of ^{87}Rb [12].

Overall, the uncertainties affecting $^{80,82,84,86}\text{Kr}$ isotope production in the *s*-process amount to as much as 66% and are largely due to nuclear physics uncertainties [13]. The situation can be improved through reliable neutron capture cross section data. The nuclear level density (NLD) and the electromagnetic decay probability, the γ -ray strength function (γ SF), are particularly important in calculating nuclear reaction cross sections [15, 16]

and have been shown to provide reliable neutron capture cross sections [17–20]. Using γ SFs and NLDs to determine capture cross sections has advantages since these properties can be obtained for any nucleus that can be sufficiently populated in a reaction from which the excitation energy can be experimentally determined. The full potential of determining capture cross sections from NLDs and γ SFs is realized by using inverse kinematic reactions. These not only make accessible a large range of radioactive species but also a vast range of previously inaccessible stable isotopes for which the manufacture of targets is problematic, due to chemical or physical properties. Measuring NLDs and γ SFs in inverse kinematic reactions provides the much needed approach to determine the electromagnetic response of nuclei, when these cannot be obtained through other techniques [21, 22].

In this Letter we report on the first measurement of the NLD and γ SF following an inverse kinematic reaction. This work lays the foundation of immense new opportunities to study statistical properties of nuclei, which were previously inaccessible, at stable and radioactive ion beam facilities. From the NLD and γ SF measured in ^{87}Kr , the astrophysical relevant $^{86}\text{Kr}(\text{n}, \gamma)$ cross section is obtained. The low-energy enhancement of the γ SF is discussed in the context of shell model calculations.

The experiment was performed with a 300-MeV ^{86}Kr beam from the Separated Sector Cyclotron facility at iThemba LABS. Polyethylene targets with 99% deuteron enrichment were bombarded with a beam intensity of ≈ 0.1 pnA for 80 hrs. Several deuterated polyethylene targets, ranging in thicknesses from 110 to 550 $\mu\text{g}/\text{cm}^2$, were used. The reactions were identified through the detection of light charged particles in two silicon ΔE -E telescopes covering scattering angles between 24° and 67° relative to the beam. The E detectors were 1 mm thick while the ΔE detectors were 0.3 and 0.5 mm thick. The dimensions of the W1-type double-sided silicon strip detectors [23] were 4.8×4.8 cm and they consisted of 16 parallel and perpendicular strips 3 mm wide with an opening angle of $\approx 1.5^\circ$ for each pixel. Suppression of δ electrons was achieved by an aluminum foil of $4.1 \text{ mg}/\text{cm}^2$ areal density which was placed in front of the ΔE detectors. The γ -rays were measured with the AFRODITE array [24], which at the time of the experiment consisted of eight collimated and Compton suppressed high-purity germanium CLOVER-type detectors mounted with four detectors each at 135° and at 90° at a distance of 21 cm from the target. Two non-collimated $\text{LaBr}_3:\text{Ce}$ detectors ($3.5'' \times 8''$) were coupled to the AFRODITE array and mounted 24 cm from the target at 45° . The detectors were calibrated using standard ^{152}Eu and ^{56}Co sources. The detector signals were processed by XIA digital electronics in time-stamped list mode with each channel self-triggered.

From the time-stamped data $\text{particle} - \gamma$ events were constructed with an offline coincidence time window of

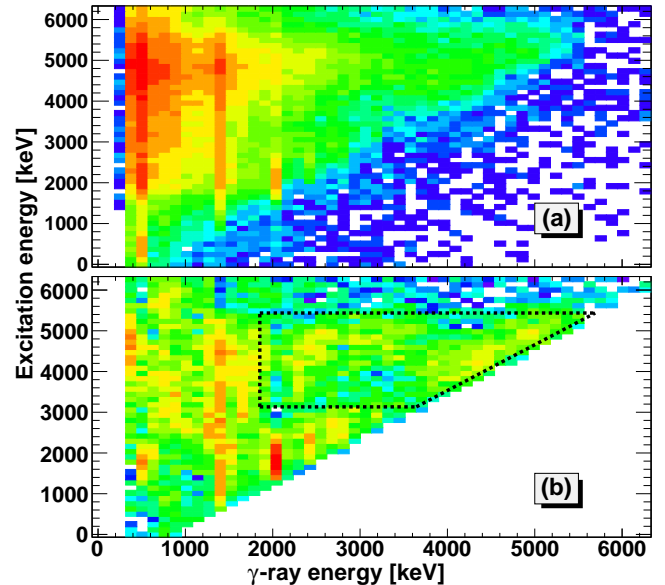


Figure 1. Raw proton- γ (a) and first-generation proton- γ (b) coincidence matrices for ^{87}Kr ($\text{LaBr}_3:\text{Ce}$ detectors only). The dashed lines enclose the area for which statistical properties were extracted.

1850 ns. From double fold events, the $p - \gamma$ coincidences were extracted by placing a gate on the protons in the particle identification spectrum. The selection of correlated events was made with a coincidence time of less than 300 ns by appropriately gating the prompt time peak. Contributions from uncorrelated events were subtracted from the data by placing off-prompt time gates. Kinematic corrections due to the reaction Q-value, recoil energy of ^{87}Kr , and the energy losses of the protons in the target and aluminum foils were applied to determine the excitation energy of the populated states. Although the target contained carbon, the kinematics for the $d(^{86}\text{Kr}, p)$ reaction compared to those of light carbon nuclei allowed for a clean extraction of the events of interest. The γ -rays in coincidence with protons were Doppler corrected on an event-by-event basis. The resulting $p - \gamma$ coincidence matrix for ^{87}Kr is shown in Figure 1(a). This matrix is unfolded [25] with response functions of the detectors extracted from a Geant4 [26] model of the detectors coupled to the AFRODITE array [27]. An iterative subtraction method, known as the first-generation method [28], is applied to the unfolded γ -ray spectra, revealing the distribution of primary γ -rays in each excitation bin (128 keV) and is shown in Figure 1(b).

The NLD at excitation energy E_x , $\rho(E_x)$, and γ -ray transmission coefficient, $\mathcal{T}(E_\gamma)$, are related to the primary γ -ray spectrum by

$$P(E_x, E_\gamma) \propto \rho(E_x - E_\gamma) \mathcal{T}(E_\gamma), \quad (1)$$

Table I. Parameters used in the normalization (see text for details).

	L	R	H
D_0 (keV)	23.30	27.25	30.5
$\sigma(S_n)$	3.475	4.012	4.486
$\langle \Gamma_\gamma \rangle$ (meV)	133	153	173

and are extracted with a χ^2 -method [21] giving the functional shape of the NLD and transmission coefficients, which are normalized to known experimental data, to retrieve the correct slope and absolute value. The extraction has been performed separately for the CLOVER and LaBr₃:Ce detectors and is limited to $3.1 < E_x < 5.4$ MeV and $E_\gamma > 1.8$ MeV of the primary γ -ray matrix where mostly statistical decay is observed, shown by the area enclosed by dashed lines in Figure 1(b).

The NLD is normalized by comparison to the known discrete levels below 2.5 MeV [29] and a constant temperature (CT) [30] interpolation between the highest data points and the neutron separation energy (S_n). The NLD at S_n is determined from the average neutron resonance spacing D_0 and the spin cutoff parameter σ in a process detailed in ref. [21]. It should be noted that our experimental resolution is of the order of ≈ 500 keV, thus a Gaussian smoothing of the discrete states has been introduced. The transmission coefficients are normalized to the average total radiative width $\langle \Gamma_\gamma \rangle$ as detailed in [31], and converted to γ SF by $f(E_\gamma) = \mathcal{T}(E_\gamma)/(2\pi E_\gamma^3)$.

To account for systematic errors introduced by the normalization process we have chosen a lower (L), recommended (R) and upper (H) set of values for the normalization. The lower value for D_0 is taken from [32], the upper value from [33], while the recommended value is the average of the two. The spin cutoff is taken as the rigid momentum of inertia [34] with a weighting factor of 0.6, 0.8 and 1.0 for L, R, and H, respectively. The total average radiative width is taken from [32, 33] and was varied within the published uncertainty. All parameters are listed in Table I.

The normalized NLDs, extracted separately for CLOVER and LaBr₃:Ce detectors, are shown in Figure 2 and are in excellent agreement with the constant temperature level density and match well with the known discrete states at lower excitation energies. The normalized γ SFs, again individually extracted for CLOVER and LaBr₃:Ce detectors, are shown in Figure 3 and are consistent with γ SFs from ⁸⁶Kr(γ, γ') [35] and ⁸⁶Kr(γ, n) [11]. A drop in the γ SFs at ~ 2.1 MeV is caused by the 2123 keV state in ⁸⁷Kr which is strongly populated in the reaction, but less through feeding from the quasi-continuum. This causes the first generation method to over subtract in the higher excitation-energy bins, causing an artificial drop in the γ SF. This effect have previously been discussed in [36]. At low energies we observe a large en-

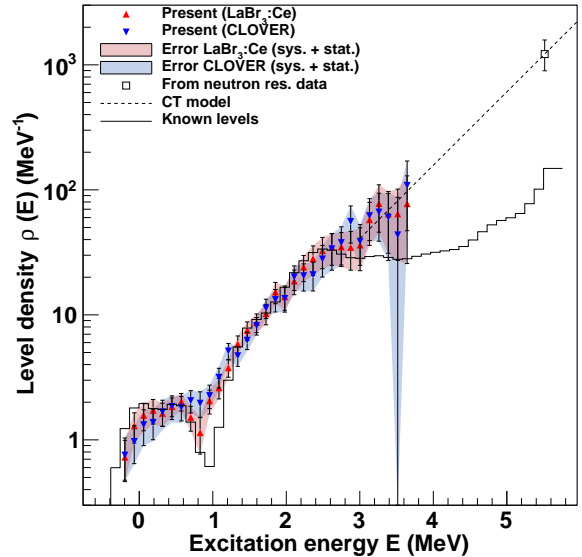


Figure 2. Normalized nuclear level densities for CLOVER (blue symbols) and LaBr₃:Ce (red symbols) detectors. The red and blue shaded bands represent the upper and lower uncertainty limit due to statistical and systematical effects (see text for details).

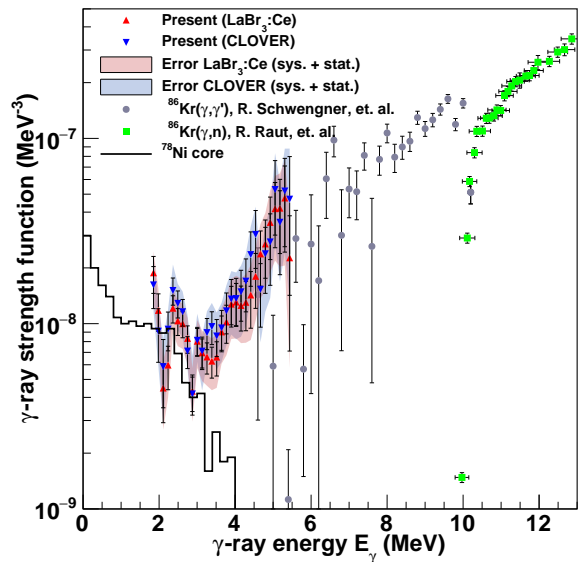


Figure 3. Gamma-ray strength function of ⁸⁷Kr for CLOVER (blue triangles) and LaBr₃:Ce (red triangles) detectors, from ⁸⁶Kr(γ, γ') (gray circles) [35] and ⁸⁶Kr(γ, n) (green squares) [11]. The red and blue shaded bands represent the upper and lower uncertainty limit due to statistical and systematical effects. The solid black line are results from a shell model calculations with ⁷⁸Ni core (see text for details).

hancement in the γ SF, similar to what has been observed in several other nuclei [19, 37–42]. Although the *upbend* has been independently confirmed [43], little is known of the origin of this feature, except that it is of dipole nature [44–46] and can have large effects on neutron capture cross sections [16].

Theoretical calculations within the shell-model framework postulate the upbend due to M1 transitions [47]. In this work, large-scale shell-model calculations of M1 γ SF were performed in the model space outside the ^{78}Ni core, containing $f_{5/2}p_{3/2}p_{1/2}g_{9/2}$ -proton and $d_{5/2}s_{1/2}d_{3/2}g_{7/2}h_{11/2}$ -neutron orbitals. The effective interaction employed here is described e.g. in Refs. [48, 49]. The diagonalization of the Hamiltonian matrix in the full configuration space was achieved using the Strasbourg shell-model code NATHAN [50]. The spin-part of the magnetic operator was quenched by a common factor of 0.75 [50]. We computed this way up to 60 states of each spin between 1/2 and 15/2 for both parities. This leads to a total of around $8 \cdot 10^4$ M1 matrix elements, among which 14822 connect states located in the energy range $E_x = 3.4 - 5.4$ MeV, as considered in the experiment. To obtain the average strength per energy interval, $\langle B(M1) \rangle$, the total transition strength was accumulated in 200 keV bins and divided by the number of transitions within these bins. The γ SF was obtained from the relation $f_{M1}(E_\gamma, E_i, J_i, \pi) = 16\pi/9(\hbar c)^{-3} \langle B(M1)(E_\gamma, E_i, J_i, \pi) \rangle \rho(E_i, J_i, \pi)$, where $\rho_i(E_i, J_i, \pi)$ is the partial level density at the energy of the initial state (E_i). The final γ SF, shown in Fig. 3, is an average of the f_{M1} 's evaluated for each spin/parity separately.

The shape of the shell-model γ SF is consistent with experimental data up to ~ 3 MeV. Since the model space does not contain all spin-orbit partners (i.e., $\nu g_{9/2}$ and $\pi f_{7/2}$ orbits) the strength above 4 MeV, due to the spin-flip transitions, can not be accounted for. On the contrary, the theoretical γ SF exhibits a peak at $E_\gamma = 0$, as in the previous shell-model calculations in this mass region [47]. The largest $B(M1)$ contributions at low γ energies in ^{87}Kr are related to transitions between close-lying negative-parity states with $\nu d_{5/2} \otimes \pi f_{5/2}^{-1}g_{9/2}^1$ and $\nu d_{5/2} \otimes \pi p_{3/2}^{-1}g_{9/2}^1$ components. The magnitude of the theoretical M1 strength seems however lower than measured in the experiment, however recent experimental results in ^{56}Fe [46] suggest a mixture of M1 and E1 radiation in the enhancement region; the addition of a non-zero E1 component at $E_\gamma \rightarrow 0$, as predicted from the shell model in Ref. [51], could thus bring a better agreement between theory and present experimental data.

In a statistical framework the $^{86}\text{Kr}(n, \gamma)$ cross-sections can be determined from the NLD, γ SF and a suitable neutron optical model potential (nOMP) for ^{87}Kr . Phenomenological nOMPs e.g. from Ref. [52] are observed to give a good agreement with the total cross-section for

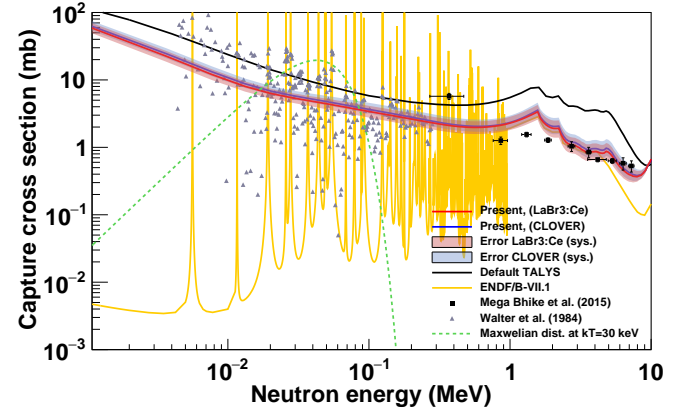


Figure 4. $^{86}\text{Kr}(n, \gamma)$ cross-sections. The red and blue lines show the TALYS result based on the LaBr₃:Ce and CLOVER results, respectively. The red and blue shaded bands represent the upper and lower uncertainty limits. The black line shows the default TALYS result and the yellow line is the evaluation of ENDF/B-VII.1 [57]. The black squares show the direct measurements of Bhike *et al.* [56] while the gray triangles show the resonance measurements of Walter *et al.* [55]. Note that the uncertainties in the Walter *et al.* is omitted for clarity, thus these data points are only intended to indicate the presence of the resonances. The MACS are obtained for the Maxwellian distribution at $kT = 30$ keV (green dashed line).

nuclei close to the valley of stability. However, due to the sensitivity of the (n, γ) cross-section on the NLD and γ SF, we expect improved results by using the experimentally measured values. For each normalization we performed calculations with the Hauser-Feshbach (HF) [53] code TALYS [54], and the optical model potential of Ref. [52]. Pre-equilibrium reactions were also taken into account. The NLD is described by the known discrete levels up to 2.5 MeV and then follows the CT formula connecting the NLD from discrete levels to the NLD at S_n . The input γ SF is an interpolation of the experimental values shown in Figure 3 with the strength below 3 MeV assumed to have M1 character. Above S_n the interpolation follows a Lorentzian curve selected such that it matches the γ SF at S_n . Figure 4 shows the comparison of the cross-sections determined from our measured NLDs and γ SFs from TALYS with the TALYS-default NLD and γ SF, direct measurements of Walter *et al.* [55] and Bhike *et al.* [56], and the evaluation of ENDF/B-VII.1 [57]. The impact of experimental NLDs and γ SFs compared to default models and parameters in TALYS is a substantial decrease in capture cross-section across all evaluated neutron energies and direct measurements above 1 MeV is well described.

The nucleosynthesis in the *s*-process is assumed to take place over a range of incident neutron energies from approximately $kT = 5$ to 100 keV [58]. Based on our results we evaluated the Maxwellian averaged cross-

sections (MACS) to be 5.4(8) mb at the standard energy of $kT = 30$ keV. This is higher compared to the evaluation of 3.4(3) mb by KADoNiS [58, 59].

To summarize, we have presented a novel method for obtaining γ SF and NLD using inverse kinematic reactions. This will allow measurements of the electromagnetic response of nuclei, and from it, the determination of astrophysically relevant capture cross sections for a large variety of previously inaccessible nuclei is possible. The γ SFs and NLDs were measured in ^{87}Kr which is of relevance for the s-process. These results were used to determine the MACS at the s-process temperature and are found to be 5.4(8) mb, somewhat higher compared to the previously evaluated MACS of 3.4(3) mb. The low-energy part of the γ SFs exhibits an enhancement which is described well with shell model calculations to be due to low-energy M1 transitions. Measuring statistical properties of nuclei from inverse kinematic reactions provides a novel and complementary foundation for exploring the limitations of the current models of statistical behavior in the nucleus. It will also allow for further constraining the uncertainties in models which are used in nuclear astrophysics and reactor physics.

This work is based on research supported by the Research Council of Norway under project Grants No. 222287, 262952 (G.M.T), 263030 (V.W.I, S.S, A.G, F.Z) and 240104 (E.S), by the National Research Foundation of South Africa, and the U.S. Department of Energy by Lawrence Livermore National Laboratory under Contract DE-AC52-07NA27344. A.C.L. gratefully acknowledges funding through ERC-STG-2014 Grant Agreement No. 637686. The authors would like to thank iThemba LABS operations for stable running conditions and John Greene (Argonne National Lab.) for providing excellent targets.

A139 (2013).

- [7] B. Singh and J. Chen, Nuclear Data Sheets **116**, 1 (2014).
- [8] E. Jagoutz, O. Jagoutz, and U. Ott, 40th Lunar and Planetary Science Conference , 1815 (2009).
- [9] M. Pignatari, R. Gallino, S. Amari, and A. Davis, Mem. S.A.It **77**, 897 (2006).
- [10] J. Harry Y. McSween and G. R. Huss, *Cosmochemistry* (Cambridge University Press, 2010).
- [11] R. Raut, A. P. Tonchev, G. Rusev, W. Tornow, C. Iliaidis, M. Lugaro, J. Buntain, S. Goriely, J. H. Kelley, R. Schwengner, A. Banu, and N. Tsoneva, Phys. Rev. Lett. **111**, 112501 (2013).
- [12] N. Nishimura, R. Hirschi, T. Rauscher, A. S. J. Murphy, and G. Cescutti, Mon. Not. R. Astron. Soc. **469**, 1752 (2017).
- [13] A. Koloczek, B. Thomas, J. Glorius, R. Plag, M. Pignatari, R. Reifarth, C. Ritter, S. Schmidt, and K. Sonnabend, At. Data Nucl. Data Tables **108**, 1 (2016).
- [14] U. Frischknecht, R. Hirschi, and F.-K. Thielemann, Astron. Astrophys. **538**, L2 (2012).
- [15] M. Arnould, S. Goriely, and K. Takahashi, Phys. Rep. **450**, 97 (2007).
- [16] A. C. Larsen and S. Goriely, Phys. Rev. C **82**, 014318 (2010).
- [17] T. A. Laplace, F. Zeiser, M. Guttormsen, A. C. Larsen, D. L. Bleuel, L. A. Bernstein, B. L. Goldblum, S. Siem, F. L. B. Garotte, J. A. Brown, L. C. Campo, T. K. Erikson, F. Giacoppo, A. Görge, K. Hadyńska-Kleś, R. A. Henderson, M. Klintefjord, M. Lebois, T. Renstrøm, S. J. Rose, E. Sahin, T. G. Tornyi, G. M. Tveten, A. Voinov, M. Wiedeking, J. N. Wilson, and W. Younes, Phys. Rev. C **93**, 014323 (2016).
- [18] A. C. Larsen, M. Guttormsen, R. Schwengner, D. L. Bleuel, S. Goriely, S. Harissopoulos, F. L. Bello Garrote, Y. Byun, T. K. Eriksen, F. Giacoppo, A. Görge, T. W. Hagen, M. Klintefjord, T. Renstrøm, S. J. Rose, E. Sahin, S. Siem, T. G. Tornyi, G. M. Tveten, A. V. Voinov, and M. Wiedeking, Phys. Rev. C **93**, 045810 (2016).
- [19] T. Renstrøm, H.-T. Nyhus, H. Utsunomiya, R. Schwengner, S. Goriely, A. C. Larsen, D. M. Filipescu, I. Gheorghe, L. A. Bernstein, D. L. Bleuel, T. Glodariu, A. Görge, M. Guttormsen, T. W. Hagen, B. V. Kheswa, Y.-W. Lui, D. Negi, I. E. Ruud, T. Shima, S. Siem, K. Takahisa, O. Tesileanu, T. G. Tornyi, G. M. Tveten, and M. Wiedeking, Phys. Rev. C **93**, 064302 (2016).
- [20] B. V. Kheswa, M. Wiedeking, J. A. Brown, A. C. Larsen, S. Goriely, M. Guttormsen, F. L. Bello Garrote, L. A. Bernstein, D. L. Bleuel, T. K. Eriksen, F. Giacoppo, A. Görge, B. L. Goldblum, T. W. Hagen, P. E. Koehler, M. Klintefjord, K. L. Malatji, J. E. Midtbø, H. T. Nyhus, P. Papka, T. Renstrøm, S. J. Rose, E. Sahin, S. Siem, and T. G. Tornyi, Phys. Rev. C **95**, 045805 (2017).
- [21] A. Schiller, L. Bergholt, M. Guttormsen, E. Melby, J. Rekstad, and S. Siem, Nucl. Instrum. Methods Phys. Res., Sect. A **447**, 498 (2000).
- [22] S. N. Liddick, A. Spyrou, B. P. Crider, F. Naqvi, A. C. Larsen, M. Guttormsen, M. Mumpower, R. Surman, G. Perdikakis, D. L. Bleuel, A. Couture, L. Crespo Campo, A. C. Dombos, R. Lewis, S. Mosby, S. Nikas, C. J. Prokop, T. Renstrom, B. Rubio, S. Siem, and S. J. Quinn, Phys. Rev. Lett. **116**, 242502 (2016).

* vetlewi@fys.uio.no

† sunniva.siem@fys.uio.no

‡ wiedeking@tlabs.ac.za

- [1] C. Arlandini, F. Käppeler, K. Wissak, R. Gallino, M. Lugaro, M. Busso, and O. Straniero, Astrophys. J. **525**, 886 (1999).
- [2] O. Straniero, R. Gallino, and S. Cristallo, Nucl. Phys. A **777**, 311 (2006).
- [3] M. Pignatari, R. Gallino, M. Heil, M. Wiescher, F. Käppeler, F. Herwig, and S. Bisterzo, Astrophys. J. **710**, 1557 (2010).
- [4] C. Abia, M. Busso, R. Gallino, I. Domínguez, O. Straniero, and J. Isern, Astrophys. J. **559**, 1117 (2001).
- [5] D. A. García-Hernández, P. García-Lario, B. Plez, F. D'Antona, A. Manchado, and J. M. Trigo-Rodríguez, Science **314**, 1751 (2006).
- [6] A. Santerne, F. Fressin, R. F. Díaz, P. Figueira, J.-M. Almenara, and N. C. Santos, Astron. Astrophys. **557**,

- [23] M. S. Ltd., *Product Catalogue*, Tech. Rep. (Micron Semiconductor Ltd., 2017).
- [24] M. Lipoglavšek, A. Likar, M. Vencelj, T. Vidmar, R. Bark, E. Gueorguieva, F. Komati, J. Lawrie, S. Maliage, S. Mullins, S. Murray, and T. Ramashidzha, Nuclear Instruments and Methods in Physics Research Section A: Accelerators, Spectrometers, Detectors and Associated Equipment **557**, 523 (2006).
- [25] M. Guttormsen, T. Tveten, L. Bergholt, F. Ingebretsen, and J. Rekstad, Nucl. Instrum. Methods Phys. Res., Sect. A **374**, 371 (1996).
- [26] S. Agostinelli, J. Allison, K. Amako, J. Apostolakis, H. Araujo, P. Arce, M. Asai, D. Axen, S. Banerjee, G. Barrand, F. Behner, L. Bellagamba, J. Boudreau, L. Broglia, A. Brunengo, H. Burkhardt, S. Chauvie, J. Chuma, R. Chytracek, G. Cooperman, G. Cosmo, P. Degtyarenko, A. Dell'Acqua, G. Depaola, D. Dietrich, R. Enami, A. Feliciello, C. Ferguson, H. Fesefeldt, G. Folger, F. Foppiano, A. Forti, S. Garelli, S. Giani, R. Giannitrapani, D. Gibin, J. G. Cadenas, I. González, G. G. Abril, G. Greeniaus, W. Greiner, V. Grichine, A. Grossheim, S. Guatelli, P. Gumplinger, R. Hamatsu, K. Hashimoto, H. Hasui, A. Heikkinen, A. Howard, V. Ivanchenko, A. Johnson, F. Jones, J. Kallenbach, N. Kanaya, M. Kawabata, Y. Kawabata, M. Kawaguti, S. Kelner, P. Kent, A. Kimura, T. Kodama, R. Kokoulin, M. Kossov, H. Kurashige, E. Lamanna, T. Lampén, V. Lara, V. Lefebure, F. Lei, M. Liendl, W. Lockman, F. Longo, S. Magni, M. Maire, E. Medernach, K. Minamimoto, P. M. de Freitas, Y. Morita, K. Murakami, M. Nagamatu, R. Nartallo, P. Nieminen, T. Nishimura, K. Ohtsubo, M. Okamura, S. O'Neale, Y. Oohata, K. Paech, J. Perl, A. Pfeiffer, M. Pia, F. Ranjard, A. Rybin, S. Sadilov, E. D. Salvo, G. Santin, T. Sasaki, N. Savvas, Y. Sawada, S. Scherer, S. Sei, V. Sirotenko, D. Smith, N. Starkov, H. Stoecker, J. Sulikimo, M. Takahata, S. Tanaka, E. Tcherniaev, E. S. Tehrani, M. Tropeano, P. Truscott, H. Uno, L. Urban, P. Urban, M. Verderi, A. Walkden, W. Wander, H. Weber, J. Wellisch, T. Weinaus, D. Williams, D. Wright, T. Yamada, H. Yoshida, and D. Zschiesche, Nuclear Instruments and Methods in Physics Research Section A: Accelerators, Spectrometers, Detectors and Associated Equipment **506**, 250 (2003).
- [27] K. C. W. Li, G. M. Tveten, and F. Zeizer, "oslo-cyclotronlab/AFRODITE: AFRODITE Response Function," (2018).
- [28] M. Guttormsen, T. Ramsøy, and J. Rekstad, Nucl. Instrum. Methods Phys. Res., Sect. A **255**, 518 (1987).
- [29] T. Johnson and W. Kulp, Nuclear Data Sheets **129**, 1 (2015).
- [30] A. Glibert and A. G. W. Cameron, Can. J. Phys. **43**, 1446 (1965).
- [31] A. Voinov, M. Guttormsen, E. Melby, J. Rekstad, A. Schiller, and S. Siem, Phys. Rev. C **63**, 044313 (2001).
- [32] S. F. Mughabghab, *Atlas of Neutron Resonances : Volume 1: Resonance Properties and Thermal Cross Sections Z= 1-60.*, sixth ed., Atlas of Neutron Resonances (Elsevier Science, 2018).
- [33] R. Capote, M. Herman, P. Obložinský, P. Young, S. Goriely, T. Belgya, A. Ignatyuk, A. Koning, S. Hilaire, V. Plujko, M. Avrigeanu, O. Bersillon, M. Chadwick, T. Fukahori, Z. Ge, Y. Han, S. Kailas, J. Kopecký, V. Maslov, G. Reffo, M. Sin, E. Soukhovitskii, and P. Talou, Nucl. Data Sheets **110**, 3107 (2009).
- [34] T. v. Egidy and D. Bucurescu, Phys. Rev. C **72**, 044311 (2005); Phys. Rev. C **73**, 049901(E) (2006).
- [35] R. Schwengner, R. Massarczyk, G. Rusev, N. Tsoneva, D. Bemmerer, R. Beyer, R. Hannaske, A. R. Junghans, J. H. Kelley, E. Kwan, H. Lenske, M. Marta, R. Raut, K. D. Schilling, A. Tonchev, W. Tornow, and A. Wagner, Phys. Rev. C **87**, 024306 (2013).
- [36] A. C. Larsen, M. Guttormsen, M. Krtička, E. Běták, A. Bürger, A. Görgen, H. T. Nyhus, J. Rekstad, A. Schiller, S. Siem, H. K. Toft, G. M. Tveten, A. V. Voinov, and K. Wikan, Phys. Rev. C **83**, 034315 (2011).
- [37] M. Guttormsen, R. Chankova, U. Agvaanluvsan, E. Algin, L. A. Bernstein, F. Ingebretsen, T. Lönnroth, S. Messelt, G. E. Mitchell, J. Rekstad, A. Schiller, S. Siem, A. C. Sunde, A. Voinov, and S. Ødegård, Phys. Rev. C **71**, 044307 (2005).
- [38] A. C. Larsen, R. Chankova, M. Guttormsen, F. Ingebretsen, S. Messelt, J. Rekstad, S. Siem, N. U. H. Syed, S. W. Ødegård, T. Lönnroth, A. Schiller, and A. Voinov, Phys. Rev. C **73**, 064301 (2006).
- [39] N. U. H. Syed, A. C. Larsen, A. Bürger, M. Guttormsen, S. Harissopoulos, M. Kmiecik, T. Konstantinopoulos, M. Krtička, A. Lagoyannis, T. Lönnroth, K. Mazurek, M. Norby, H. T. Nyhus, G. Perdikakis, S. Siem, and A. Spyrou, Phys. Rev. C **80**, 044309 (2009).
- [40] A. C. Larsen, I. E. Ruud, A. Bürger, S. Goriely, M. Guttormsen, A. Görgen, T. W. Hagen, S. Harissopoulos, H. T. Nyhus, T. Renstrøm, A. Schiller, S. Siem, G. M. Tveten, A. Voinov, and M. Wiedeking, Phys. Rev. C **87**, 014319 (2013).
- [41] A. Simon, M. Guttormsen, A. C. Larsen, C. W. Beausang, P. Humby, J. T. Burke, R. J. Casperson, R. O. Hughes, T. J. Ross, J. M. Allmond, R. Chyzh, M. Dag, J. Koglin, E. McCleskey, M. McCleskey, S. Ota, and A. Saastamoinen, Phys. Rev. C **93**, 034303 (2016).
- [42] B. V. Kheswa, M. Wiedeking, F. Giacoppo, S. Goriely, M. Guttormsen, A. Larsen, F. B. Garrote, T. Eriksen, A. Görgen, T. Hagen, P. Koehler, M. Klintefjord, H. Nyhus, P. Papka, T. Renstrøm, S. Rose, E. Sahin, S. Siem, and T. Tornyi, Phys. Lett. B **744**, 268 (2015).
- [43] M. Wiedeking, L. A. Bernstein, M. Krtička, D. L. Bleuel, J. M. Allmond, M. S. Basunia, J. T. Burke, P. Fallon, R. B. Firestone, B. L. Goldblum, R. Hatarik, P. T. Lake, I.-Y. Lee, S. R. Lesher, S. Paschalidis, M. Petri, L. Phair, and N. D. Scielzo, Phys. Rev. Lett. **108**, 162503 (2012).
- [44] A. C. Larsen, N. Blasi, A. Bracco, F. Camera, T. K. Eriksen, A. Görgen, M. Guttormsen, T. W. Hagen, S. Leoni, B. Million, H. T. Nyhus, T. Renstrøm, S. J. Rose, I. E. Ruud, S. Siem, T. Tornyi, G. M. Tveten, A. V. Voinov, and M. Wiedeking, Phys. Rev. Lett. **111**, 242504 (2013).
- [45] A. C. Larsen, M. Guttormsen, N. Blasi, A. Bracco, F. Camera, L. C. Campo, T. K. Eriksen, A. Görgen, T. W. Hagen, V. W. Ingeberg, B. V. Kheswa, S. Leoni, J. E. Midtbø, B. Million, H. T. Nyhus, T. Renstrøm, S. J. Rose, I. E. Ruud, S. Siem, T. G. Tornyi, G. M. Tveten, A. V. Voinov, M. Wiedeking, and F. Zeiser, Jour. Phys. G Nucl. and Part. Phys. **44**, 064005 (2017).
- [46] M. D. Jones, A. O. Macchiavelli, M. Wiedeking, L. A. Bernstein, H. L. Crawford, C. M. Campbell, R. M. Clark, M. Cromaz, P. Fallon, I. Y. Lee, M. Salathe, A. Wiens, A. D. Ayangeakaa, D. L. Bleuel, S. Bottoni, M. P. Carpenter, H. M. Davids, J. Elson, A. Görgen, M. Guttormsen, R. V. F. Janssens, J. E. Kinnison, L. Kirsch, A. C. Larsen, T. Lauritsen, W. Reviol, D. G. Sarantites,

- S. Siem, A. V. Voinov, and S. Zhu, Phys. Rev. C **97**, 024327 (2018).
- [47] R. Schwengner, S. Frauendorf, and A. C. Larsen, Phys. Rev. Lett. **111**, 232504 (2013).
- [48] M. Czerwiński, T. Rzaca-Urban, W. Urban, P. Bączyk, K. Sieja, B. M. Nyakó, J. Timár, I. Kuti, T. G. Tornyi, L. Atanasova, A. Blanc, M. Jentschel, P. Mutti, U. Köster, T. Soldner, G. de France, G. S. Simpson, and C. A. Ur, Phys. Rev. C **92**, 014328 (2015).
- [49] J. Litzinger, A. Blazhev, A. Dewald, F. Didierjean, G. Duchêne, C. Fransen, R. Lozeva, K. Sieja, D. Verney, G. de Angelis, D. Bazzacco, B. Birkenbach, S. Botttoni, A. Bracco, T. Braunroth, B. Cederwall, L. Corradi, F. C. L. Crespi, P. Désesquelles, J. Eberth, E. Ellinger, E. Farnea, E. Fioretto, R. Gernhäuser, A. Goasduff, A. Görgen, A. Gottardo, J. Grebosz, M. Hackstein, H. Hess, F. Ibrahim, J. Jolie, A. Jungclaus, K. Kolos, W. Korten, S. Leoni, S. Lunardi, A. Maj, R. Menegazzo, D. Mengoni, C. Michelagnoli, T. Mijatovic, B. Million, O. Möller, V. Modamio, G. Montagnoli, D. Montanari, A. I. Morales, D. R. Napoli, M. Niikura, G. Pollarolo, A. Pullia, B. Quintana, F. Recchia, P. Reiter, D. Rosso, E. Sahin, M. D. Salsac, F. Scarlassara, P.-A. Söderström, A. M. Stefanini, O. Stezowski, S. Szilner, C. Theisen, J. J. Valiente Dobón, V. Vandone, and A. Vogt, Phys. Rev. C **92**, 064322 (2015).
- [50] E. Caurier, G. Martínez-Pinedo, F. Nowacki, A. Poves, and A. P. Zuker, Rev. Mod. Phys. **77**, 427 (2005).
- [51] K. Sieja, Phys. Rev. Lett. **119**, 052502 (2017).
- [52] A. Koning and J. Delaroche, Nucl. Phys. A **713**, 231 (2003).
- [53] W. Hauser and H. Feshbach, Phys. Rev. **87**, 366 (1952).
- [54] A. J. Koning, S. Hilaire, and M. C. Duijvestijn, in *International Conference on Nuclear Data for Science and Technology 2007* (EDP Sciences, Les Ulis, France, 2008) pp. 2–5.
- [55] G. Walter, *Neutron density and temperature of the weak s-process component (original: Temperatur und Neutronendichte der schwachen Komponente des s-Prozesses)*, Tech. Rep. KFK-3706 (Kernforschungszentrum Karlsruhe, 1984) data retrieved from the EXFOR database, file EXFOR 22037.010.
- [56] M. Bhike, E. Rubino, M. E. Gooden, Krishchayan, and W. Tornow, Phys. Rev. C **92**, 014624 (2015).
- [57] M. Chadwick *et al.*, Nucl. Data Sheets **112**, 2887–2996 (2011).
- [58] Z. Bao, H. Beer, F. Käppeler, F. Voss, K. Wissak, and T. Rauscher, At. Data Nucl. Data Tables **76**, 70–154 (2000).
- [59] I. Dillmann, AIP Conf. Proc. (2006), 10.1063/1.2187846, online at <http://www.kadonis.org>.